Journal of Magnetism and Magnetic Materials 369 (2014) 96–100

Contents lists available at ScienceDirect

Journal of Magnetism and Magnetic Materials

journal homepage: www.elsevier.com/locate/jmmm

Energy-imbalance mechanism of domain wall motion induced by propagation spin waves in finite magnetic nanostripe

Jinrong Zhu, Zhaoyan Han, Yuanchang Su*, Jingguo Hu [1]

College of Physics Science and Technology, Yangzhou University, Yangzhou 225002, People's Republic of China

ARTICLE INFO

Article history:
Received 1 March 2014
Received in revised form
26 May 2014
Available online 12 June 2014

Keywords:
Domain wall motion
Spin wave
Energy-imbalance mechanism
Micromagnetic simulation

ABSTRACT

The mechanism of the domain wall (DW) motions induced by spin wave in finite magnetic nanostripe is studied by micromagnetic simulations. We find that the spin-wave induced DM motions are always accompanied by an energy imbalance between two sides of the DW. The DW motion can be attributed to the expansion of the low-energy-density area and the contraction of the high-energy-density area. The energy imbalance strongly depends on whether the spin wave passes through the DW or is reflected by the DW. In the area of the spin wave propagation, the energy density increases with the time. However, in the superposition area of the incident spin wave and the reflected spin wave, the energy density decreases with the increasing of the time. It shows that this energy imbalance can be controlled by tuning the frequency of the spin wave. Finally, the effect of the damping parameter value is discussed.

1. Introduction

Current-induced domain wall (DW) motion [1], which has potential application to the next generation data storage [2] and logic devices [3], has been intensively studied in recent years. The motion of domain walls due to spin transfer torque of electrons has been well studied experimentally [4–6] and theoretically [7–10]. Recently, it was found that a spin wave (SW) excited by a microwave field can also drive a DW motion [11–13]. Furthermore, by assistance of SW, the current-induced DW motion can be improved [14,15]. Burn and Atkinson [16] reported that a structural control of spin wave emission can suppresses Walker breakdown [17–19] and high DW velocity is maintained over a wide field range. By micromagnetic simulations, it was shown that the spin waves may cause the DW to move in the same or opposite direction to that of the SW propagation, which is strongly dependent on the transmission coefficient of the SWs [20–23]. Moreover, the transmission coefficient of SW passing through the DW strongly depends on the frequency of the SW [20,21]. Namely, in the low-frequency region, there is an large reflection of SWs, and the DW moves in the same direction to that of SWs propagation. While in the high-frequency region, the transmission coefficient is very close to a unity, and the DW motion in the opposite direction to that of SWs propagation [21,22]. However, the underlying mechanism of the spin-wave induced DW motions is not very clear. Hinzke et al. and Yan et al. suggested that the mechanism of DW motion is a magnonic spin-transfer torque mechanism [24,25]. But this mechanism can only explain the DW propagate in the opposite direction to that of the SWs.

In this paper, the mechanism of the spin-wave induced DW motions in finite magnetic nanostripe is studied by micromagnetic simulations. In finite stripe, the SW may be reflected by the DW or by the boundary of the stripe. When the transmission coefficient of SW passing through the DW is small, a superposition area of the incident SW and the reflected SW (reflected by the DW) forms in the left side of the DW. In this case, a small passing SW propagates in the right side of the DW. When the transmission coefficient is close to a unity, only the incident SW propagates in the left side, and the superposition area of the passing SW and the reflected SW (reflected by the boundary of the stripe) forms in the right side. In the simulations, we show that the different patterns of SW propagation in two sides of the DW lead to an energy imbalance. Namely, the energy density increases with the time in the area of the SW propagation, while the energy density decreases with the increasing of the time in the superposition area. The DW motion can be attributed to the expansion of the low-energy-density area and the contraction of the high-energy-density area. By this energy-imbalance mechanism, all the characteristics of spin-wave-induced DW motion can be explained.

2. Model

The finite magnetic nanostripe used in this paper is 640 nm long in the x direction, 50 nm wide in the y direction and 10 nm thick, as shown in Fig. 1. A transverse wall is placed at the center

* Corresponding author. Tel.: +86 0514 87975466.
E-mail addresses: ycsu@yzu.edu.cn (Y. Su), jghu@yzu.edu.cn (J. Hu).
[1] Tel.: +86 0514 87970587.

http://dx.doi.org/10.1016/j.jmmm.2014.06.015
0304-8853/

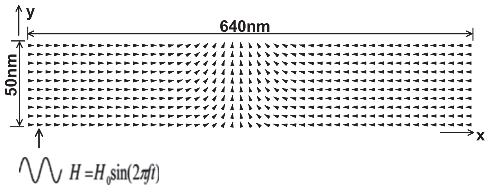

Fig. 1. Illustration of the model nanostripe. A head-to-head transverse wall is placed at the center (x=320 nm) of the stripe. $H(t)$ is the external field that excites the SW.

(x=320 nm) of the stripe and relaxed to stable. A external harmonic sinusoidal field along y axis is applied at the left-end edge of the stripe to excite SWs. In such finite stripe, sizeable distortions may occur in left-end and right-end edges of the stripe, which may influence the excitation of the SW. In order to avoid the distortions, the left-end and right-end edges of the stripe are pinned. In simulations, the unit cell size is 4 nm × 4 nm × 10 nm, the saturation magnetization $M_s = 8.6 \times 10^5$ A/m and the exchange stiffness $A = 1.3 \times 10^{-11}$ J/m. In the study, we used the generalized Landau-lifshitz-Gilbert (LLG) equation to describing the magnetization dynamics. It is

$$\frac{\partial \mathbf{M}}{\partial t} = -\gamma \mathbf{M} \times \mathbf{H}_{eff} + \alpha \mathbf{M} \times \frac{\partial \mathbf{M}}{\partial t} \quad (1)$$

where **M** is the unit magnetization vector. $\mathbf{H}_{eff}$ is the effective field including the exchange coupling field, the magnetostatic field and the external field. γ is the gyromagnetic ratio and α is the Gilbert damping parameter. In this paper, we choose α=0.01 and $\gamma = 2.21 \times 10^5$ m/As. Other damping parameter values α=0.02, 0.03 are also discussed.

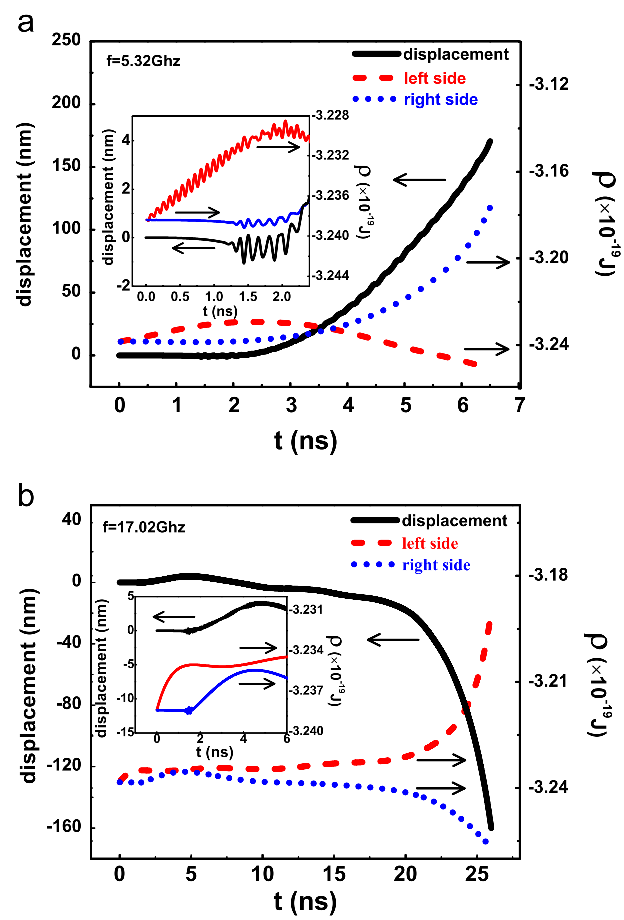

Fig. 2. The displacement of the DW as well as the average energy densities ρ in left and right side areas as functions of time t with SW frequencies of (a) f=5.32 GHz and (b) 17.02 GHz. The insets are the amplified scales of the displacement and the energy density. Damping parameter α = 0.01.

3. Results and discussions

Fig. 2 shows the displacement of the DW as well as the average energy densities ρ in left and right side areas as functions of time t with SW frequencies of f=5.32 GHz and f=17.02 GHz. As shown in Fig. 2(a), for low frequency f=5.32 GHz, the DW moves in the same direction to that of the SW propagation. In the region of $t < 1.35$ ns, where the SW has not propagated to the DW, the average energy density in left side increases and the average energy density in right side does not change. When $t > 1.35$ ns, most part of SW is reflected by the DW and a very small part of SW passes through the DW. In this region, the average energy density in left side firstly increases then decreases, while the average energy density in right side increases. For high frequency of f=17.02 GHz, the DW moves in the opposite direction to that of SWs propagation, as shown in Fig. 2(b). In the region of $t < 1.35$ ns, it appears to be similar to that of low frequency f=5.32 GHz. In the region of $t > 1.35$ ns, the average energy density in left side increases, while the average energy density in right side firstly increases then decreases. The change of the average energy density mainly results from the pattern of SW propagation, which will be explained below. Importantly, Fig. 2 indicates that the energy imbalance between two sides of the DW may be the underlying mechanism for the spin-wave induced DW motions. In order to decrease the total energy of the system, the low-energy-density area expands and the high-energy-density area contracts, which lead to DW motions.

Fig. 3 shows the y-axis component of the magnetic moment M_y as a function of x at different times. It demonstrates well the DW motions and the SW excitations at low frequency f=5.32 GHz and high frequency of f=17.02 GHz, as shown in Fig. 3(a) and (b), respectively. Some example structures of micromagnetic spins detailing the evolution of DW structure with SW excitations are shown in Fig. 4. The result shows that the DW motions and the SW excitations are similar to that of Fig. 3. By the way, in the magnetic nanostripe used in this paper, the propagation velocity of the SWs is about $u = 218.5$ m/s. The wavelength of SW can be calculated by $\lambda = u/f$, e.g., λ=41.07 nm for f=5.32 GHz and λ=12.84 nm for f=17.02 GHz, respectively.

Noted that the steady-state motion [22,24] with a constant velocity is not found in such a finite stripe, namely the DW moves with an acceleration stage. In order to obtain more quantitative information on the relationship between SW frequency and DW motion, the average velocity is calculated.

Fig. 5 shows the average velocity v of DW (during a displacement duration $\Delta X = 160$ nm) as a function of the SW frequencies. It shows that the average velocity decreases rapidly with the increasing of frequency. In the low-frequency region of $f < 17$ GHz, the DW moves in the same direction to that of the SW propagation ($v > 0$). At a frequency of about f=14 GHz, there is a sudden increase in the velocity compared with neighboring frequencies. When $f > 17$ GHz, the velocity becomes negative ($v < 0$), namely the DW moves in the opposite direction to that of SW propagation. This result is in qualitative agreement with that of Ref. [22].

In order to understand the results shown in Fig. 2, we focus on two typical positions (x=250 nm and x=400 nm) located in different sides of the initial DW (x=320 nm). The average magnetic moments within these two positions are timely calculated.

Fig. 6 shows the average magnetic moment M_y and the energy density ρ as a function of time t with low frequency f=5.32 GHz. For the left-side position of x=250 nm, it can be divided into three